STRUCTURE OF A TWO-DIMENSIONAL TURBULENT BOUNDARY LAYER OVER A SUBMERGED CYLINDRICAL PROTURBERANCE

Jacob George
Department of Aerospace and Ocean Engineering
Virginia Tech, Blacksburg, VA 24061-0203
george@aoe.vt.edu

Roger L. Simpson
Department of Aerospace and Ocean Engineering
Virginia Tech, Blacksburg, VA 24061-0203
simpson@aoe.vt.edu

ABSTRACT

Detailed individual measurements are made in the downstream flow-fields of three cylindrical protuberances of heights, h^+, non-dimensionalized by friction velocity (U_τ) of the approach turbulent boundary layer (BL), of 23, 46 and 92 using a special fine-measurement-volume (30 microns diameter) three-orthogonal-velocity-component fiber-optic Laser Doppler Velocimeter (LDV) system. The trailing legs of the horseshoe vortex formed in front of the single element causes an increased downwash, bringing greater momentum fluid closer to the wall. For all cases, this "sweep" type motions causes higher Reynolds stresses ($\overline{v^2}$, $\overline{w^2}$ and $-\overline{uv}$) downstream of the element. Further, this greater momentum fluid close to the wall leads to greater skin-friction drag. However, for the lowest element, the skin-friction drag is lower than that for the undisturbed approach boundary layer at locations further downstream from the element.

INTRODUCTION

The present study is a subset of a larger study dealing with the effect of sparse distributions of cylindrical roughness elements on turbulent boundary layers. For this, it's important to find the effect of an isolated roughness element. To study the effect of roughness, one can envision a distribution of similar individual elements. The shape of the roughness element strongly influences the strength and size of the horseshoe vortex structure. It is doubtful that surface shape irregularities that are smaller than the smallest smooth-wall scale $12\nu/U_\tau$ have much influence. For the present experiment, three individual cylindrical protuberances with the same diameter but with different heights, close to the order of smooth-wall scales, are used. Little literature is available on the turbulent structure of such small scale protuberances. Recently, Fontaine and Deutsch (1996) found that sweeps and ejections were retarded in the near-wall region downstream of a "gaussian" shaped spike, of h^+=16.4 and d^+ (non-dimensionalized base diameter) = 13, leading to lower near-wall $-\overline{uv}$ Reynolds stress and local wall shear. In the present experiments, the reduction in wall shear is seen only in the lowest cylindrical element. The experimental results are also expected to provide a test case for DNS and LES studies.

EXPERIMENTAL SET-UP AND MEASUREMENT TECHNIQUE

Measurement of mean velocities and fluctuating quantities (Reynolds stresses and the triple products) were made using the three-orthogonal-velocity-component fiber-optic LDV system which is a sub-system of the five-velocity-component fiber-optic LDV system (Ölçmen and Simpson, 1995a). The data reduction techniques have also been discussed in the same paper. The nearly spherical probe volume had an effective diameter of 30 microns. Oil-flow visualizations are carried out using the technique described by Ölçmen and Simpson (1995b). The measurements were carried out in the Virginia Tech Aerospace and Ocean Engineering Department Low Speed Boundary Layer Tunnel at a nominal speed of $27.5\,m/s$. The undisturbed boundary layer (also referred to as reference BL) has a thickness of 39.6 mm with Re_θ of 7300 and friction velocity (U_τ) of $0.95\,m/s$. Three separate experiments were performed with three cylinders of heights (h) of 0.015" (0.38 mm), 0.030" (0.76 mm) and 0.060" (1.52 mm), with each having a diameter (d) of 0.078" (1.98 mm). Measurement locations for each of these cases are the same and are shown in Fig. 1. The uncertainty in the results are same as those reported in George and Simpson (2000). Traversed lengths along the streamwise (x) direction and the spanwise (z) direction are non-dimensionalized by the diameter (d) of the element. Normal to the wall (y) lengths and all the velocities are non-dimensionalized by the length scale (ν/U_τ)

and velocity scale (U_τ) of the reference BL, respectively and are denoted by a superscript, '+'.

RESULTS AND DISCUSSION

Results for the mean streamwise velocity U^+ Vs y^+ (Fig. 2) show that the profiles for the h = 0.015" case at various x/d are similar to the reference profile. Slightly higher near-wall values are seen in h = 0.030" and 0.060" cases, with the latter case showing the highest values. Higher speed fluid along the centerline (z =0) is also corroborated by the flow visualization photographs (Fig. 3). High scouring (along the centerline) is due to the increased downwash behind the element, on account of the vortex pair bringing greater momentum fluid closer to the wall leading to higher wall shear. This fact is reflected in the values of the wall shear obtained and is presented as a ratio of local wall shear (τ_w) to the reference BL wall shear (τ_{wo}), both along the streamwise (Fig. 4a) and spanwise (Fig. 4b) directions. However, there is an exception in the h = 0.015" case, at the downstream locations (x/d =20 and 40). For added confidence, values of this ratio (τ_w/τ_{wo}) at locations slightly off-center at these two x/d locations is shown in table 1.

The lower shear (as compared to the reference BL) at the centerline is probably due to the lower "strength" of the "sweeping" motion and that it might be just counteracting the "ejection" motion. Such a similar finding of lower wall shear was seen in the flow field downstream of a "gaussian" spike by Fontaine and Deutsch (1996). They also show the wall shear values to recover to smooth wall values at x^+ =350. However, this is not true in this case (h = 0.015") even at x/d = 40 which corresponds to x^+ =4810. The downstream lengths of dark scours on oil flows persist to approximately 65 diameters for the h = 0.015" case; 85 diameters for h = 0.030"; and 100 diameters for the h = 0.060". The flow visualization pictures (Fig. 3) also reveal higher deposits away from the centerline along spanwise (z) direction, indicating lower shear as compared to the centerline. The spanwise variations of wall shear, presented for all cases at x/d =10, show that it first increases away from the centerline and then gradually decreases. Lower shear is attributed to less mixing at those regions, due to the presence of the vortex pair. Higher shear closer to the centerline is of course due to the downwash due to the vortex pair and to a lesser extent due to the mild acceleration of the converging fluid behind the protuberance as it convects downstream within the confines of the two counter-rotating vortices.

To determine wall shear, the friction velocity (U_τ) was calculated from a refined determination of the measurement volume location relative to the wall, obtained by a least squares fit of the viscous sublayer mean velocity profile, $Q = c_1 y + c_2 y^4$, with $Q = \sqrt{U^2 + W^2}$ and c_1 and c_2 as coefficients. The curve was fit through $Q = 0$ and $y = 0$. Using only the data for $y^+ < 10$, an iterative process was used to maximize the curve fit correlation coefficient by shifting the y values by Δy. At least 5 points were used to obtain the curve fits. Using the curve fit, the wall shearing stress $\tau_w/\rho = \nu(\partial Q/\partial y)\big|_{wall} = U_\tau^2$ is given by $c_1 \upsilon$.

Figure 5 shows the streamwise variation of the streamwise normal stress, $\overline{u^2}/U_\tau^2$ versus y^+ along the downstream centerline. In all cases, peaks are seen at location directly behind the element and are seen below the element heights. Closers to the wall, the stress levels are higher at locations nearer to the element for h = 0.015" and 0.030" cases. The near-wall stress levels are higher than the undisturbed values at all locations in the h =.060" case. However, the peak values at downstream locations are lower than the undisturbed values for all cases.

Figures 6, 7 and 8 show the streamwise variations of $\overline{v^2}/U_\tau^2$, $\overline{w^2}/U_\tau^2$ and $\overline{uv}/U_\tau^2$ with y^+, respectively. At or below the element heights, all cases show much higher stress levels than the reference values, with values progressively increasing with increasing element height. This shows that a larger element creates a vortex structure of greater strength, thereby augmenting higher "sweeping" motions leading to higher stress levels. It may be noted that the peaks in the individual profiles of $\overline{v^2}$ and $\overline{w^2}$ are located slightly below the element height and the peak in the $\overline{uv}$ profiles occurs at or about the element height.

Figure 9 shows the contours of turbulent kinetic energy (TKE), $\frac{1}{2}\overline{q^2}$, normalized on U_τ, along with the vectors of the diffusion velocities $V_q = \overline{vq^2}/\overline{q^2}$ and $W_q = \overline{wq^2}/\overline{q^2}$ at x/d =10. The turbulent vortex core is seen to move lower and away from the centerline with increasing element height. The increase in TKE values is rather gradual with increase in element height. TKE is seen to diffuse down the gradient, but the diffusion velocity vectors are not generally normal to the TKE contours near or around the vortex core. The posts also greatly increase the diffusion velocities. This vector is a representation of the direction of the occasional large-scale motions of turbulence.

Figures 10 and 11 show the streamwise variations of $\overline{u^2v}/U_\tau^3$ and $\overline{u^3}/U_\tau^3$ with y^+, respectively. Gentle negative peaks in the profiles of $\overline{u^2v}$ are seen close to the wall. At these peak locations, the corresponding values of $\overline{u^3}$ are positive, indicating that the $\overline{u^2}$ momentum is carried towards the wall with the faster moving fluid in the flow direction, a "sweeping" motion. Most of the near-wall region is dominated by sweeps, with sweeping motions increasing with increase in the size of the element. The presence of horseshoe vortices producing sweep type motions is consistent with the observed behavior of $\overline{u^2v}$. Away from the wall and closer to the element height, the profiles of $\overline{u^2v}$ change sign with peaks seen just under the element height, indicating the transport of $\overline{u^2}$ momentum away from the wall, an "ejection" motion.

CONCLUSIONS

From the results and observations, a schematic model may be made. As an upstream boundary layer approaches a single element, a horseshoe vortex is formed in front of the element (Fig. 12) and its trailing legs pass around the sides of the element, forming a pair of counter-rotating streamwise vortices. The diameter of the vortex trailing legs are of the order of the height of the single element. Measurements reveal that this horseshoe vortex pair causes an increased downwash behind the element, with greater momentum fluid being brought down closer to the wall behind the element. This "sweep" type motion dominates the near wall structure leading to higher Reynolds stresses ($\overline{v^2}$, $\overline{w^2}$ and $-\overline{uv}$). Furthermore, this greater momentum near the wall results in greater skin-friction drag. An upwash occurs on the outer edges (George, 2001) of the horseshoe vortex pair, which ejects low-speed fluid away from the wall, also increasing the Reynolds shearing stress. It is clear that such wall disturbances propagate outward from the wall into the outer region along real hyperbolic characteristic lines, which have been measured for smooth wall flows. The approach velocity gradient and the shape and height of the roughness element strongly influence the strength and size of the horseshoe vortex structure leads to the increased downwash behind the element.

Acknowledgements

This work was supported by the US Office of Naval Research under N00014-99-1-0228, Dr. L. P. Purtell, Program Manager. The authors are indebted to Mr. Gwibo Byun for help with the measurements.

References

Fontaine, A. A., and Deutsch, S., 1996, "Structure of near wall turbulence downstream of a wall mounted protrusion: an interesting Reynolds stress suppression phenomena", Experiments in Fluids, vol. 20, pp. 365-376.

George, J., and Simpson, R. L., 2000, "Some effects of sparsely distributed three-dimensional roughness elements on two-dimensional turbulent boundary layers", AIAA Paper 2000-0915.

George, J., 2001, "Structure of three-dimensional turbulent boundary layers with sparsely distributed roughness", Ph.D. dissertation, Department of Aerospace and Ocean Engineering, Virginia Polytechnic Institute and State University. (in progress).

Ölçmen, S. M., and Simpson, R. L., 1995a, "A five-velocity-component laser-Doppler velocimeter for measurements of a three-dimensional turbulent boundary layer", Measurement Sciences Technology, vol. 6, pp. 702-716.

Ölçmen, S. M., and Simpson, R. L., 1995b, "An experimental study of a three-dimensional pressure-driven turbulent boundary layer", Journal of Fluid Mechanics, vol. 290, pp. 225-262.

z/d =	-0.139	0	0.139
x/d =20	0.99	0.94	1.01
x/d =40	0.97	0.95	0.98

Table 1 : Off-center values of τ_w/τ_{wo} at x/d =20 and 40, for h = 0.015".

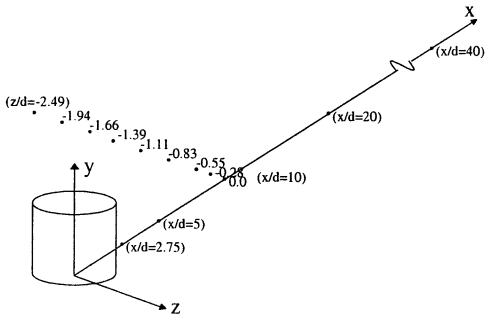

Figure 1 : Measurement locations

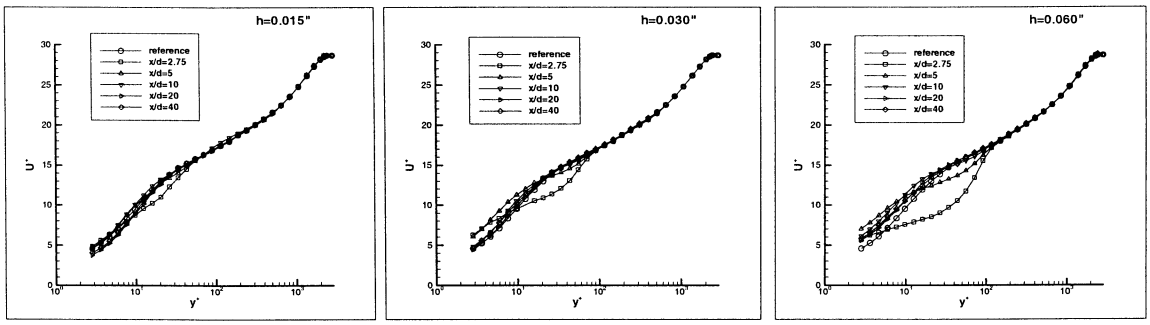

Figure 2 : U^+ versus y^+, streamwise mean velocity profiles along the centerline

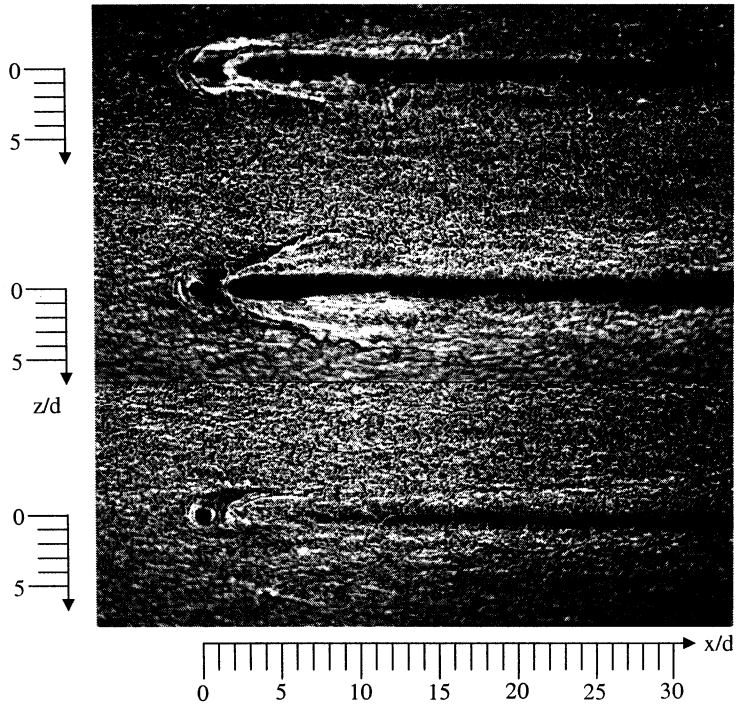

Figure 3 : Top-view of surface oil flow over isolated cylindrical elements; h =0.060" (top), 0.030" (middle), 0.015" (bottom)

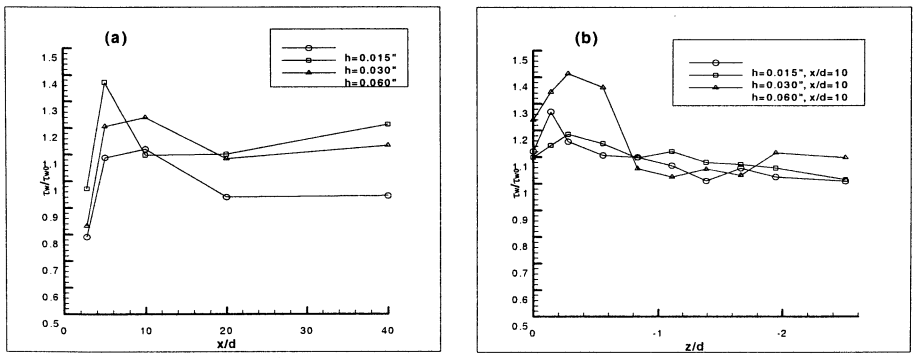

Figure 4 : Normalized wall shear (τ_w/τ_{wo}) : (a) Centerline Streamwise variation, (b) Spanwise variation at x/d =10

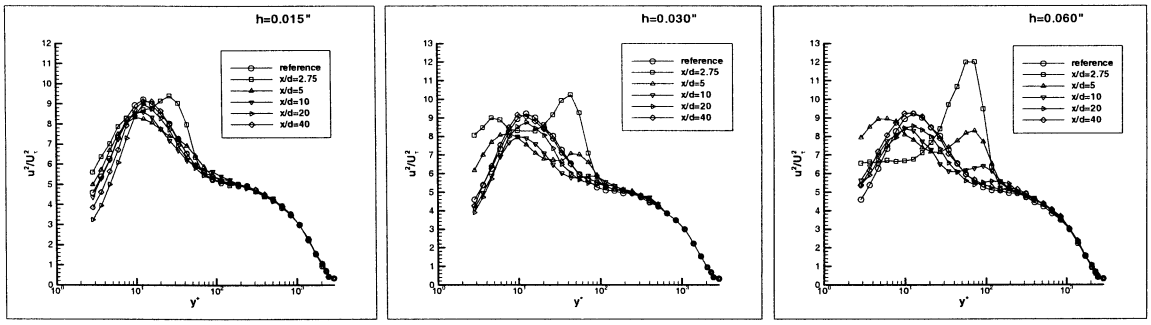

Figure 5 : $\overline{u^2}/U_\tau^2$ versus y^+, streamwise turbulent normal stress profiles along the centerline

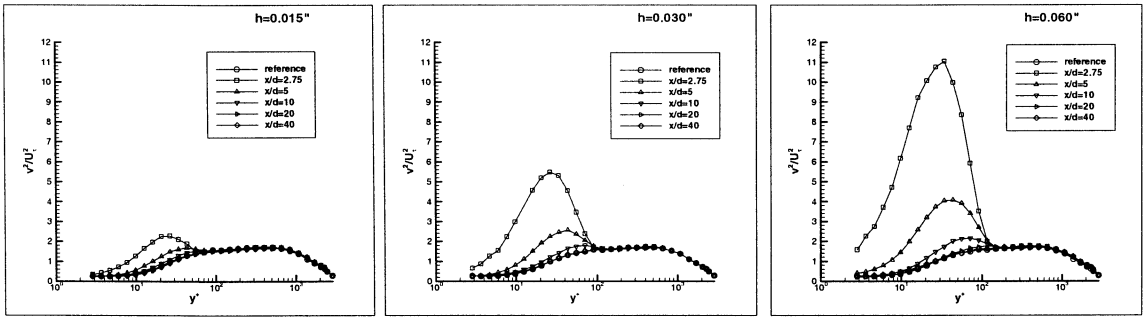

Figure 6 : $\overline{v^2}/U_\tau^2$ versus y^+, normal to wall normal stress profiles along the centerline

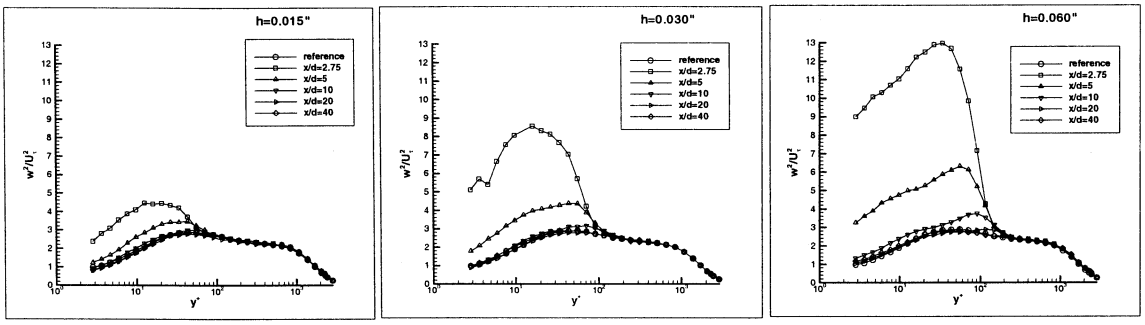

Figure 7 : $\overline{w^2}/U_\tau^2$ versus y^+, spanwise turbulent normal stress profiles along the centerline

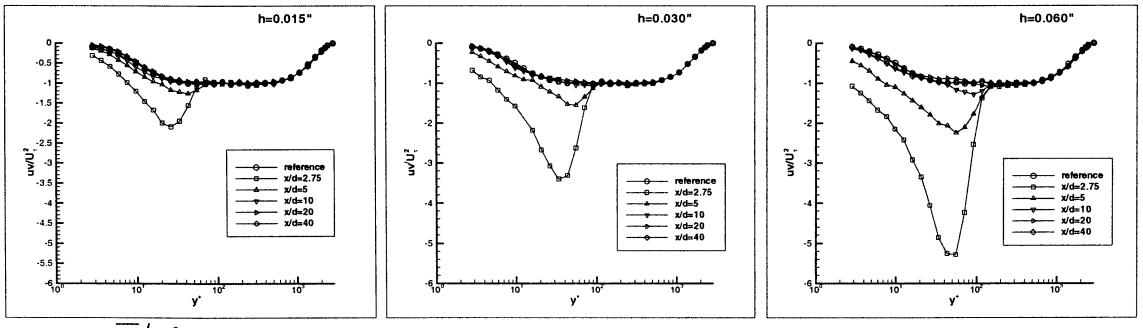

Figure 8 : $\overline{uv}/U_\tau^2$ versus y^+, streamwise Reynolds shearing stress profiles along the centerline

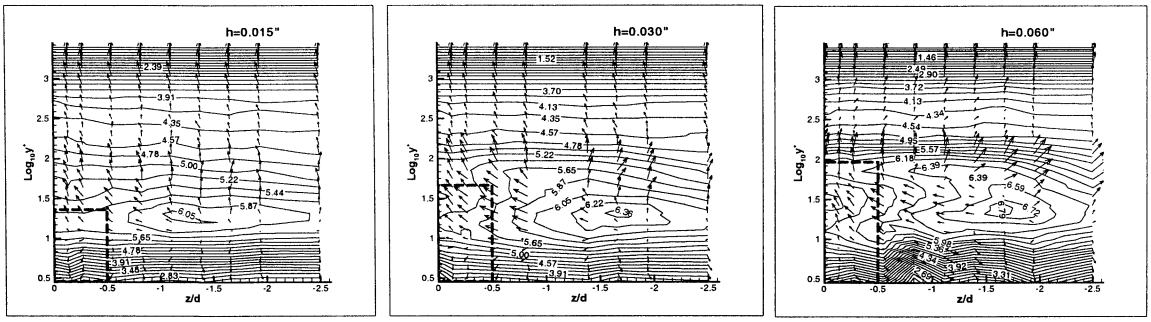

Figure 9 : The TKE and the TKE diffusion velocity at x/d =10: Contours of $\frac{1}{2}\overline{q^2}/U_\tau^2$ and vectors of V_q and W_q ; single elements shown as dashed lines

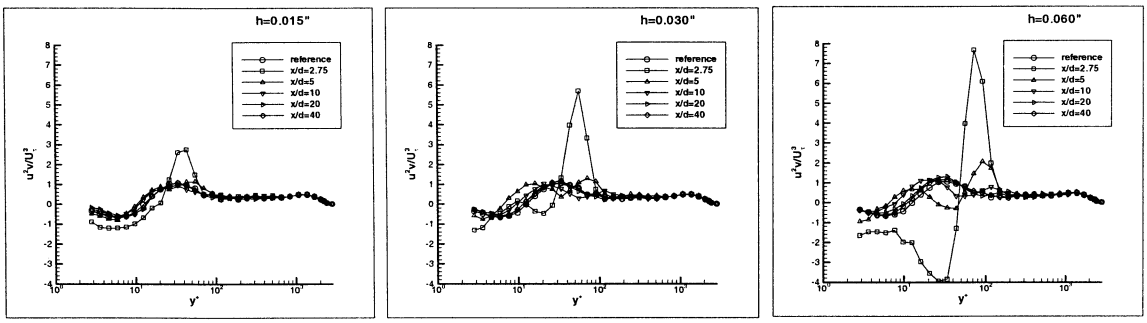

Figure 10 : $\overline{u^2v}/U_\tau^3$ versus y^+ profiles along the centerline

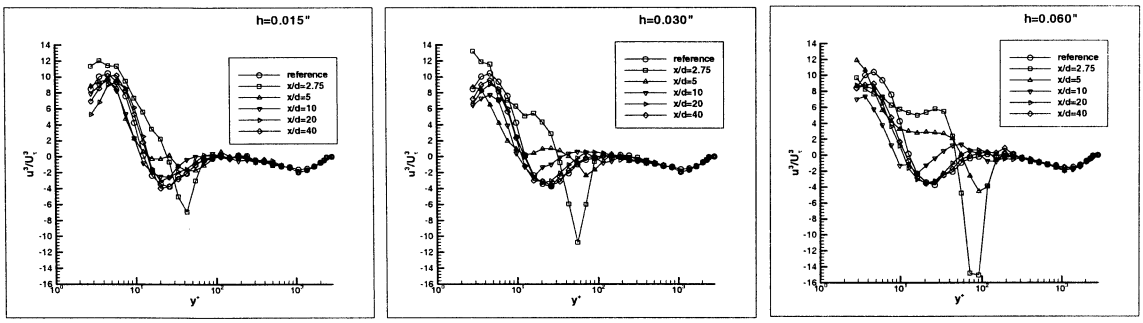

Figure 11 : $\overline{u^3}/U_\tau^3$ versus y^+ profiles along the centerline

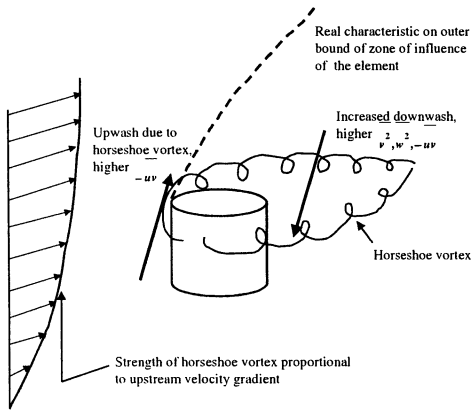

Figure 12 : Schematic of the role of the horseshoe vortices in increasing the Reynolds stresses downstream of the element. Note the outgoing real characteristic from the single element.